

## Surface superconducting states in a yttrium hexaboride single crystal in a tilted magnetic field

This article has been downloaded from IOPscience. Please scroll down to see the full text article.

2010 J. Phys.: Condens. Matter 22 095701

(<http://iopscience.iop.org/0953-8984/22/9/095701>)

View [the table of contents for this issue](#), or go to the [journal homepage](#) for more

Download details:

IP Address: 129.252.86.83

The article was downloaded on 30/05/2010 at 07:23

Please note that [terms and conditions apply](#).

# Surface superconducting states in a yttrium hexaboride single crystal in a tilted magnetic field

M I Tsindlekht<sup>1</sup>, V M Genkin<sup>1</sup>, G I Leviev<sup>1</sup> and N Yu Shitsevalova<sup>2</sup>

<sup>1</sup> The Racah Institute of Physics, Hebrew University of Jerusalem, 91904 Jerusalem, Israel

<sup>2</sup> Institute for Problems of Materials Science, National Academy of Sciences of Ukraine, 03680 Kiev, Ukraine

Received 26 November 2009, in final form 25 January 2010

Published 17 February 2010

Online at [stacks.iop.org/JPhysCM/22/095701](http://stacks.iop.org/JPhysCM/22/095701)

## Abstract

We present the results of an experimental study of the nucleation of superconductivity at the surface of a single-crystal YB<sub>6</sub> in a tilted dc magnetic field. The developed experimental approach allowed us to measure  $H_{c3}$  at each side of the sample as a function of the angle between the dc magnetic field and the surface. Experiment showed that the ratio  $H_{c3}/H_{c2} \approx 1.28$  when the dc field became perpendicular to the surface while the expected value of this ratio is 1. This sharp distinction with theory cannot be ascribed to the surface roughness.

(Some figures in this article are in colour only in the electronic version)

## 1. Introduction

Shortly after Saint-James and de Gennes' prediction of surface superconductivity [1] many experiments have confirmed their basic idea. Resistive and permeability measurements at low frequencies [2–6] showed that, in parallel to the surface dc field, the ratio  $H_{c3}/H_{c2}$  is close to the theoretical value 1.695. The value of  $H_{c3}$  depended on the angle  $\theta$  between the dc field and the sample surface and decreased as this angle was increased. The critical surface current, defined as the current at which the sample exhibits a finite resistance, also decreased with increasing  $\theta$ . The ac response of surface superconducting states (SSS) has characteristic features such as the loss maximum in the intermediate fields  $H_{c2} < H_0 < H_{c3}$ , low frequency dispersion and nonlinearity at very low excitation levels [6]. Concurrently, a number of theoretical models for the calculation of the critical current in the SSS were published (see, for example, references in [6]). Agreement between the theoretical models and experimental data was not satisfactory. Therefore, attempts were made to develop a more sophisticated model of the SSS, in particular, a model of the surface vortices was elaborated [7–11]. In these models, the surface vortices could move only if the surface current exceeds some critical value. Actually this is a variant of the critical state model which was applied to the SSS. When the dc magnetic field is parallel to the sample surface, the normal component is zero and the density of the surface vortices is zero. It was proposed [7]

that, due to the surface roughness, locally the dc magnetic field has a normal component which provides some finite density of surface vortices. The experiments [7, 8] demonstrated that the surface critical current dramatically depends on the surface roughness and the angle between the dc magnetic field and the surface. AC losses in the critical state model have a threshold character with respect to the amplitude of excitation [6]. All the above-mentioned experiments were performed on polycrystalline metals or alloys. In spite of all this research an adequate theory that could explain all peculiarities of the low frequency dynamics of the SSS, for example, frequency dispersion, has not been proposed as yet. In addition, recent experiments did not reveal any vanishing of losses with decreasing ac amplitude [12, 14] and showed that the nonlinear response could not be described by perturbation theory [14].

Resistive and torque measurements [2, 3, 5] demonstrated that SSS did not exist ( $H_{c3}/H_{c2} = 1$ ) if the dc field is perpendicular to the surface, as was predicted by theory [1]. On the other hand, ac measurements [4] showed that in a perpendicular field the transition to a superconducting state takes place in fields above  $H_{c2}$ . It was assumed that there was a superconducting network of negligible volume that was not detected in any bulk effects [4]. The measurements of the resistance of the niobium strip in a dc magnetic field perpendicular to large sample faces in [13] revealed that the superconductivity in the sample could exist up to the field

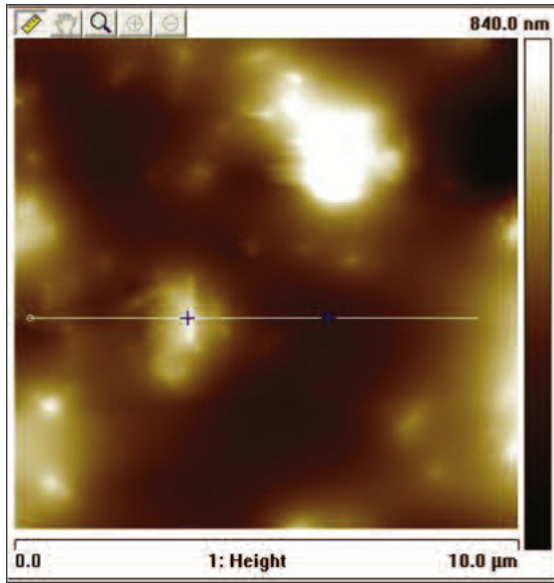


Figure 1. AFM image of the YB<sub>6</sub> sample surface.

$H_0 = 1.76H_{c2}$ . But the contribution of the lateral sample sides for which the dc field was parallel to the surface is unclear from these experimental data.

In this paper we present results of a systematic investigation of the angular dependence of  $H_{c3}$  for a YB<sub>6</sub> single crystal. The developed experimental approach permitted us to separate the contribution from each surface of the sample. We found that  $H_{c3}/H_{c2} = 1.28$  in a dc magnetic field perpendicular to the surface. Numerical analysis of the influence of the surface roughness on the  $H_{c3}$  showed that this could not account for this large ratio  $H_{c3}/H_{c2}$ .

## 2. Experimental details

We have measured the ac response of a YB<sub>6</sub> single crystal with size 10 mm × 3 mm × 1 mm which was cut from a large crystal. Sample surfaces were mechanically and then chemically polished. Roughness of the large sample surfaces were measured by an atomic force microscope (AFM), model Nanoscope Dimension 3100 (Veeco Co.). This AFM has a planar resolution of about 5 nm and a vertical resolution of about 0.05 nm. Five AFM 35 × 35 μm<sup>2</sup> images were obtained from each large sample face. The spectral RMS roughness amplitude did not exceed 100 nm. But we found that at some points the roughness height was about 1 μm. Figure 1 demonstrates an example of such images. The spectral RMS roughness amplitude along the straight line in this figure is about 80 nm. DC magnetization curves were measured by a commercial SQUID magnetometer.

The ac response at the fundamental frequency, and the third harmonic signal, were taken concurrently using the pickup coil method [15]. A block diagram of the experimental set-up is shown in figure 2. The ac field was supplied by two identical drive coils that were connected in series with the load resistor. Drive coils are driven by a low frequency generator (LFG). The sample was inserted into one of the

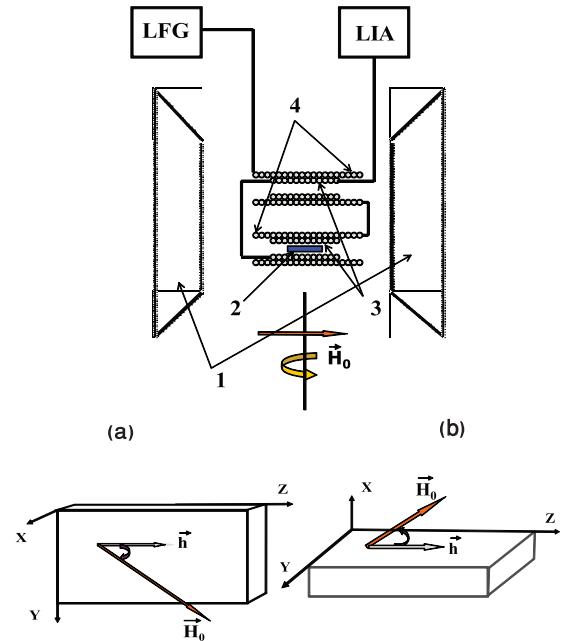


Figure 2. Block diagram of the experimental set-up. LFG—low frequency generator, LIA—lock-in amplifier, 1—electromagnet poles, 2—sample, 3—pickup coils and 4—drive coils. Inset (a)—sketch of the dc field rotation in XZ plane. Inset (b)—sketch of the dc field rotation in YZ plane.

pickup coils. Empty pickup coils are balanced without any external circuits. The unbalanced signal as a function of the external parameters was measured by a lock-in amplifier (LIA). A small unbalanced signal of the empty pickup coils was measured and subtracted as well. A small probe coil (not shown in figure 2) was employed for ac amplitude calibration. The electromagnet was rotated around the vertical axis, figure 2. Fourier analysis of the time-dependent magnetization in an ac field  $h(t) = 2h_0 \cos(\omega t)$  yields an expression of the form  $m(t) = h_0 \sum_n \chi_n(\omega) \exp(-in\omega t)$ . The frequency and amplitude of the applied ac field were 565 Hz and 0.05 Oe, respectively. This frequency has been chosen by taking into account our experimental constraints and results of [14] that the frequency dispersion was not important for bringing about the superconducting transition. We assume that in zero dc field at low temperatures the losses are negligible and the ac in-phase component,  $\chi'_1$ , does not depend on frequency and equals  $-1/4\pi$ . This assumption permitted us to get the values of  $\chi_1$  and  $\chi_3$  in absolute units in finite dc fields. The absence of frequency dispersion in zero dc field was verified experimentally.

Two experimental configurations were chosen for the parallelepiped-shaped sample. The first one (G1) is when the dc field rotates in the XZ plane (figure 2, inset (a)) and the second one (G2) is when the dc field rotates in the YZ plane (figure 2, inset (b)). With the first configuration, G1, the dc field remains parallel to the small faces (XZ plane) for any angle  $\theta$  while with G2 the field is always parallel to the wide faces (YZ plane). The angle  $\theta$  is the angle between the Z axis and the direction of the dc magnetic field. In all measurements the ac field was parallel to the

Z axis. The measured ac response for these two configurations was different and therefore it permitted us to calculate the ac response for each sample side as a function of the dc field inclination angle  $\theta$  because for each angle we have two sets of experimental data and two values of the surface current (due to symmetry, currents on opposite sides are equal to each other). This procedure has been described below and the value of the surface current at each side was found.

### 3. Experimental results

YB<sub>6</sub> is an isotropic BCS superconductor. It has some advantages due to the experimentally well-defined  $H_{c2}$  as one can see in the inset to figure 3(a). Properties of YB<sub>6</sub> were measured with high accuracy in [14, 16] where it was found that  $T_c \approx 7.2$  K, correlation length at  $T = 0$ ,  $\xi_0 \approx 45$  nm, and the Ginzburg–Landau (GL) parameter  $\kappa \approx 3.5$ .

Figure 3(a) presents in- and out-of-phase components of  $\chi_1$  for  $T = 4.2$  K as a function of the dc field for some angles  $\theta$  between the wide sample side ( $YZ$  plane) and the dc field while it remained parallel to the narrow side ( $XZ$  plane). Figure 3(b) shows the corresponding results for another orientation of the dc field when it was parallel to the wide sides and had an angle to the narrow sides (see inset (b) in figure 2). One can readily see that for these two dc field orientations (G1 and G2) both  $\chi_1'(H_0)$  and  $\chi_1''(H_0)$  are well distinguished.

### 4. Discussion

The raw experimental data (figures 3(a) and (b)) contain the contribution of four sample sides to the ac response. In order to separate the response from each side we used the following procedure. Let us consider the ac response of the long rectangular slab in the normal state with a thin superconducting sheath (of a thickness of several coherence lengths) at the surface (inset to figure 3(b)). The ac field in the bulk can be found from the solution of the two-dimensional equation:

$$\frac{\partial^2 h_z}{\partial x^2} + \frac{\partial^2 h_z}{\partial y^2} + \frac{2i}{\delta^2} h_z = 0, \quad (1)$$

where  $\delta = c/\sqrt{2\pi\sigma\omega}$  is the normal skin depth and  $\sigma$  is a normal conductivity. We took into account that an applied ac field has only one Z component, and neglected the small demagnetization factor along the Z axis  $\approx 0.045$ . The surface sheath is carrying a surface current  $J_s$ , the value of which depends on the value of the dc field and its orientation with respect to the surface. This current screens the inner part of the sample and, neglecting the thickness of this sheath, we can write the boundary condition for equation (1) at each sample side in the form

$$h_z^{si} = h_0 + 4\pi J_{si}/c, \quad (2)$$

where  $h^{si}$  is the amplitude of the ac field on the boundary between the normal sample core and the surface sheath at the  $i$ th sample side, and  $J_{si}$  is the surface current at the  $i$ th side. Indexes  $i = 1, 2$  correspond to the wide sides while  $i = 3, 4$

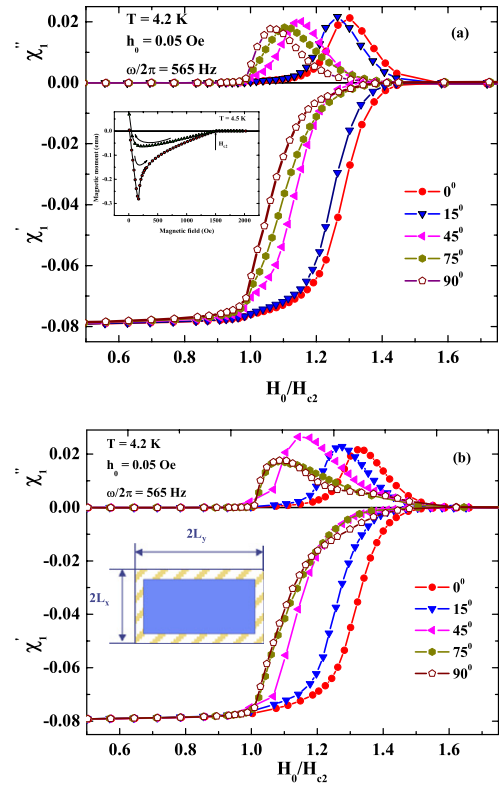


**Figure 3.** Field dependence of  $\chi_1'$  and  $\chi_1''$  for different angles  $\theta$ . Panel (a):  $\chi_1$  for orientation of the dc field that is parallel to the narrow sample side and has an angle  $\theta$  to the wide side (rotation in  $XZ$  plane). The magnetization curve is presented in the upper inset. Panel (b):  $\chi_1$  for orientation of the dc field that is parallel to the wide sample side and has an angle  $\theta$  to the narrow side (rotation in  $YZ$  plane). The inset shows the sample cross section. The darkened area shows (not to scale) the sample part in a normal state and the light colored part in a superconducting state, respectively.

correspond to the narrow sides. The straightforward solution of equation (1) is

$$h_z = \sum_{n=1,3,\dots} \frac{4}{\pi n} \sin(\pi n/2) \cos(\pi n x/2L_x) \times \left\{ \frac{h^{s1} \sinh[k_n(L_y + y)]}{\sinh[2k_n L_y]} + \frac{h^{s2} \sinh[k_n(L_y - y)]}{\sinh[2k_n L_y]} \right\} + \sum_{n=1,3,\dots} \frac{4}{\pi n} \sin(\pi n/2) \cos(\pi n y/2L_y) \times \left\{ \frac{h^{s3} \sinh[q_n(L_x + x)]}{\sinh[2q_n L_x]} + \frac{h^{s4} \sinh[q_n(L_x - x)]}{\sinh[2q_n L_x]} \right\}, \quad (3)$$

where

$$k_n^2 \equiv (\pi n/2L_x)^2 - 2i/\delta^2, \quad q_n^2 \equiv (\pi n/2L_y)^2 - 2i/\delta^2,$$

$L_x$  and  $L_y$  are sample sizes in the  $XY$  plane ( $L_x > L_y$ ). The average ac magnetic field,  $\bar{h}_z \equiv \frac{1}{L_x L_y} \int_0^{L_x} \int_0^{L_y} h_z dx dy$ , is

$$\bar{h}_z = h_z^{s1} Z_1 + h_z^{s3} Z_2, \quad (4)$$

where

$$Z_1 = 8 \sum_{m=1,3}^{\infty} \frac{\tanh(k_m L_y)}{\pi^2 m^2 k_m L_y}$$

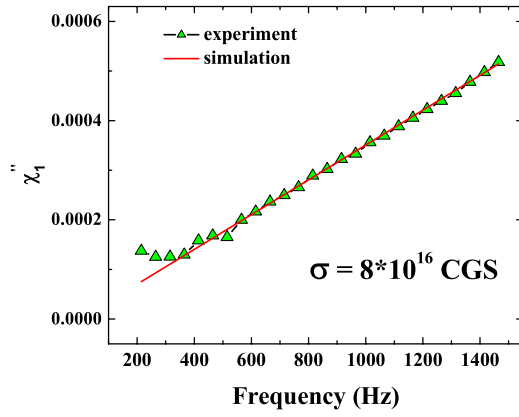


**Figure 4.** Frequency dependence of  $\chi_1''$  for the sample in a normal state at  $T = 7.5$  K.

and

$$Z_2 = 8 \sum_{m=1,3}^{\infty} \frac{\tanh(q_m L_x)}{\pi^2 m^2 q_m L_x}.$$

It was taken into account that, due to the symmetry,  $h^{s1} = h^{s2}$  and  $h^{s3} = h^{s4}$ . The observed magnetic susceptibility is

$$\chi_1 = (\bar{h}_z/h_0 - 1)/4\pi. \quad (5)$$

Using these expressions and the experimental data one can find the surface currents at each side of the sample. If  $\vec{H}_0$  lies in the  $XZ$  plane and the angle between dc field and  $OZ$  axis is  $\theta$ :

$$1 + 4\pi \tilde{\chi}_1(\theta) = Z_1 h_z^{s1}(\theta)/h_0 + Z_2 h_z^{s2}(\theta)/h_0, \quad (6)$$

while if  $\vec{H}_0$  lies in the  $YZ$  plane and forms the same angle with the  $OZ$  axis, then

$$1 + 4\pi \tilde{\tilde{\chi}}_1(\theta) = Z_1 h_z^{s2}(\theta)/h_0 + Z_2 h_z^{s1}(\theta)/h_0, \quad (7)$$

where  $\tilde{\chi}_1(\theta)$  and  $\tilde{\tilde{\chi}}_1(\theta)$  are the measured susceptibilities for the G1 and G2 configurations of the dc field, respectively. For any given angle and dc magnetic field we can find from these two equations both  $h_z^{s1}(\theta)$  and  $h_z^{s2}(\theta)$  and calculate the surface currents from equation (2). The bulk conductivity in a normal state  $\sigma$  can be found from the ac response at temperatures  $T > T_c$ . Under these conditions  $h^{s1} = h^{s3} = h_0$  at  $T > T_c$ . Figure 4 demonstrates the frequency dependence of  $\chi_1''$  at  $T = 7.5$  K. This experiment was carried out on the set-up described in [17]. Mapping these data by equation (6) we obtain  $\sigma = 8 \times 10^{16}$  CGS. This value is in good agreement with the result of [16] for the same sample (it was cut from the same ingot).

Experimental results can be presented in terms of the surface current,  $J_s$ , normalized in such a way that the complete shielding by the surface current corresponds to  $J_s = -1$  while for the surface sheath in a normal state  $J_s = 0$ . Surface current data in figures 5(a) and (b) correspond to the dc magnetic field rotated in and out of the surface, respectively. If the dc magnetic field is parallel to the narrow faces, figure 5(a) corresponds to the current at wide faces while figure 5(b) to narrow faces and vice versa, if the dc magnetic field is

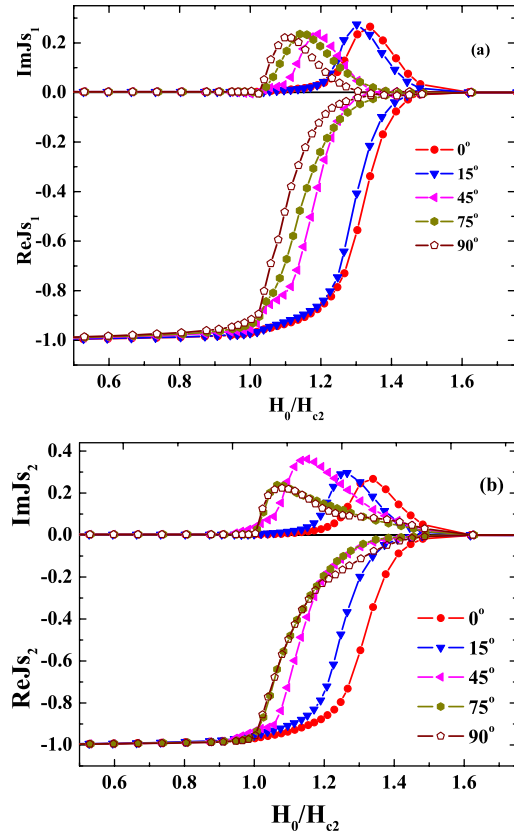


**Figure 5.** Panel (a): field dependence of the  $J_s$  in the case when the dc field makes an angle with the surface. Panel (b): field dependence of the  $J_s$  when both dc and ac fields are parallel to the surface but make some angle with each other.

parallel to wide faces, figure 5(a) shows the current at narrow faces while figure 5(b) is for wide faces. We see that in the perpendicular dc field the superconducting transition at the surface takes place at  $H_0 > H_{c2}$ . The observed response at the third harmonic confirms this conclusion also. The third harmonic vanishes if the dc field becomes smaller than  $H_{c2}$ . The nonlinear response disappears simultaneously with the disappearance of the surface current in an increased dc field. Moreover, the nonlinear response depends on the orientation of the dc field, as is shown in figures 6(a) and (b). The orientation of the dc and ac magnetic fields here was the same as for figures 3(a) and (b). For the third harmonic data we did not perform the procedure of separating the response from each sample side. However, the first harmonic data show that the wide sides provide the largest contribution to the ac response. This is why the dependence of  $|\chi_3|$  on the angle shown in figure 6(a) reflects the dependence of the nonlinear response by SSS on the angle between a parallel to the surface ac and dc fields. When  $\vec{H}_0$  is parallel to the surface, the observed onset of the superconducting transition does not depend on the angle between the ac and dc fields, as was expected, figure 5(b), but the value of  $J_s$  depends on this angle. Figure 7 demonstrates the angular dependence of the surface current  $J_s$  for several dc fields. This dependence is nonmonotonic at low dc fields. Detailed discussion of the angular dependence of  $J_s$  will be reported in our forthcoming publications.



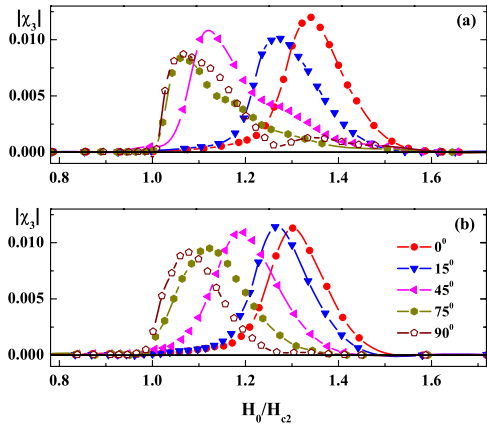


**Figure 6.** Field dependence of  $|\chi_3|$  for different configurations of the dc field. Panel (a): the case when the dc field remains parallel to the  $YZ$  sample surface but forms some angle with respect to the ac field. Panel (b): the case when the dc field remains parallel to the  $XZ$  sample plane.

The existence of the SSS in a perpendicular dc field for  $H_0 > H_{c2}$  can be ascribed to surface roughness. It is well known that the surface roughness strongly affects the properties of the SSS [7, 8, 10, 12, 13]. Thus  $H_{c3}$  depends on the surface roughness [7, 8, 12, 13]. SSS are localized in the surface layer with a thickness of a few coherence lengths. For a rough surface the dc field is not parallel to the local normal even if it is perpendicular to the surface and one could expect the manifestation of SSS in fields  $H_0 > H_{c2}$ . The value of  $H_{c3}$  could be calculated from the first GL equation for a given magnetic field:

$$\ln(T_c/T)\{-\Psi + |\Psi|^2\Psi\} + (i\vec{\nabla} + \vec{a})^2\Psi = 0, \quad (8)$$

with boundary conditions  $\frac{d\Psi}{dn}|_S = 0$  at the surface. Here  $\Psi = \Delta/\Delta_0$  is the dimensionless order parameter,  $\Delta_0$  is the order parameter at a given temperature and zero dc field,  $\vec{a} = 2e\vec{A}/\hbar c$ ,  $\vec{A}$  is a vector potential ( $\text{curl}\vec{A} = \vec{H}_0$ ), the length unit is  $\xi_0$  and the coherence length at  $T = 0$ , and  $\vec{n}$  is a local outer normal to the sample surface. For a really rough surface this is a 3D equation and in order to simplify the problem we considered only the 2D version where the surface profile depended only on one direction ( $Z$  axis). Because the analytical solution is not possible for a rough surface profile we used the numerical method. Equation (8) had been transformed to

$$\begin{aligned} & \ln(T_c/T)\{-\Psi(n, m) + |\Psi(n, m)|^2\Psi(n, m)\} \\ & - \frac{\Psi(n+1, m) + \Psi(n-1, m) - 2\Psi(n, m)}{dx^2} \\ & - \frac{\Psi(n, m-1) + \Psi(n, m+1) - 2\Psi(n, m)}{dz^2} \\ & + (H_z n dx - H_x m dz - k)^2\Psi(n, m) = \gamma \frac{d\Psi(n, m)}{dt} \end{aligned}$$

at the 2D grid with steps  $dx$  and  $dz$ . Here  $H_x$  and  $H_z$  are the components of the external dc field and  $k$  is a constant. The value of  $k$  is chosen from the condition that the stationary nontrivial solutions of this set of equations could be found for

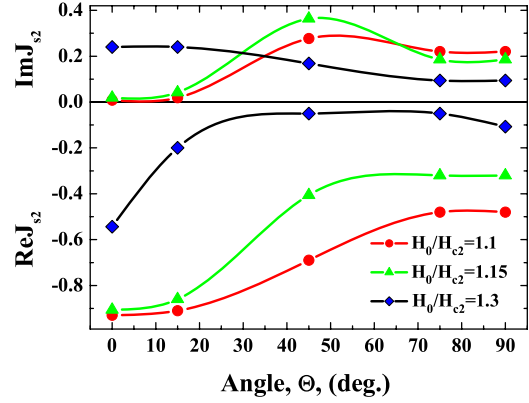


**Figure 7.** Real and imaginary parts of the surface current as a function of the angle between the ac and dc fields for several dc fields. Both fields are parallel to the surface.

a given dc field. The maximal value of  $H_0$  for a given angle, for which such a solution could be found, was considered as  $H_{c3}$  at this angle. Actually, a grid with  $10^4$  points was used. Calculations were performed for several types of surface roughness, for a model with sinusoidal surface profile, figure 8(a), and for the actual surface profile that was measured by an atomic force microscope (AFM), figure 8(c).

The shape of the superconducting nucleus near the rough surface is shown for illustration in figures 8(b) and (d). Figure 8(b) demonstrates the results of the numerical calculation of the spatial distribution of the order parameter near the surface with a sinusoidal roughness, with period  $m \times \xi_0$  and amplitude  $n \times \xi_0$ , while figure 8(d) shows the order parameter for the surface profile measured by the AFM. The angle between the dc field direction and the sample surface equals  $45^\circ$  in both cases. Careful analysis of these figures shows that a superconducting phase nucleates near such points where the angle between the dc field and the local normal is close to  $\pi/2$ .

Figure 9 shows both the experimental and calculated  $H_{c3}/H_{c2}(\theta)$  dependence for several models of surface roughness. Experimentally  $H_{c3}$  was determined using the procedure proposed by Rollins and Silcox in 1967 [6] and based on the appearance of the field dependence of the ac response. Curve (A) corresponds to the ideally smooth surface; (B) to a sinusoidal model with period  $20 \times \xi_0$  and amplitude  $1 \times \xi_0$ ; (C) for a period  $10 \times \xi_0$  and amplitude  $5 \times \xi_0$  and curve (D) corresponds to the actual surface profile with the steepest roughness. This profile was measured by AFM and it was chosen for  $H_{c3}$  calculations as the most likely for nucleation of the superconducting phase. In case B, when the surface is relatively smooth  $H_{c3}/H_{c2} = 1.56$  for the dc field parallel to the surface. This is in good agreement with the experimental value of 1.57. However, the calculated  $H_{c3}$  decreases with angle and for  $\theta = \pi/2$   $H_{c3}/H_{c2} = 1$  while the experimental value is 1.28 (figure 9). For steeper roughness  $H_{c3}/H_{c2} \approx 1.25$  at angles close to  $\pi/2$  (curve C). This ratio fits well the experimental value of 1.28 for a perpendicular dc field. However, curve C was calculated for a very steep roughness with inclination about  $67^\circ$  that was not observed

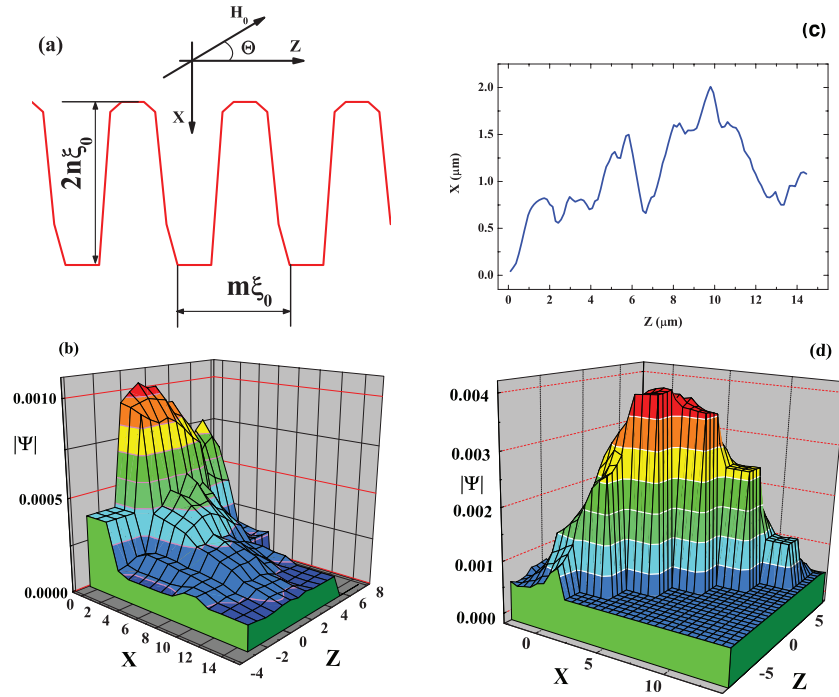


**Figure 8.** Panel (a): the model profile of the rough surface and orientation of the dc magnetic field. Panel (b): calculated order parameter (absolute value) for SSS for the model surface in the dc field  $H > H_{c2}$  and  $\theta = 45^\circ$ . Panel (c): measured by the AFM actual profile of the surface. Panel (d): the calculated order parameter near the surface for actual surface profile ( $\theta = 45^\circ$ ).  $\xi_0$  is the unit length for (b) and (d) panels. See the text.

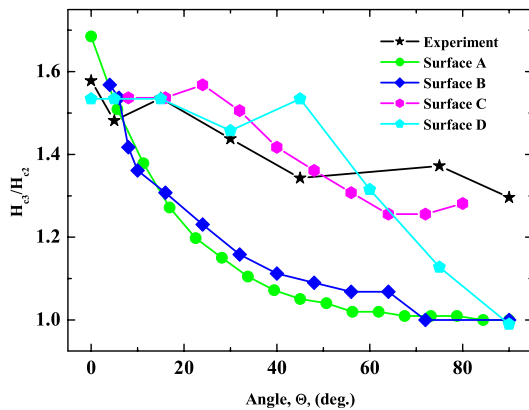


**Figure 9.** The angular dependence of the  $H_{c3}/H_{c2}$  ratio: experiment and calculations for several models of the surface roughness. Curve A corresponds to the ideally smooth surface; curve B to a sinusoidal surface with  $m = 20$  and  $n = 1$ ; curve C to the model surface with  $m = 10$  and  $n = 5$ ; and curve D to the profile measured by AFM. See text.

for our sample by AFM. The highest surface inclination of the measured profile is about  $45^\circ$ . In accordance with the A-type curve, figure 9, for this surface inclination the ratio  $H_{c3}/H_{c2}$  should be about 1.1, but not 1.28. We see that the actual surface roughness could not yield such a large value of  $H_{c3}/H_{c2}$  in a perpendicular dc field. Another hypothesis, that there is a superconducting network in the bulk which is not seen by dc measurements [4] at  $H_0 > H_{c2}$ , leads to the requirement that the bulk has to have normal conductivity which is approximately 100 times larger than was measured.

## 5. Conclusions

We have studied the low frequency ac response of a  $YB_6$  single crystal in a tilted dc magnetic field. The developed approach has permitted us to obtain the value of the ac surface current at each side of the sample. The  $H_{c3}$  angular dependence when the dc field rotates out of the plane was obtained. The experiment showed that in the dc field perpendicular to the surface the transition to the superconducting state took place in a field  $H_0 \approx 1.28H_{c2}$ . We demonstrated also that the induced ac surface current is a function of the angle between the ac and dc fields when both fields are parallel to the large sample surface. The measurement of the surface roughness by AFM showed that such a large  $H_{c3}$  could not be ascribed, at first glance, to the roughness as a possible reason. A new experimental study of the ac response in a tilted magnetic field on samples with different roughness should be carried out. These studies will provide an answer to the question: is the sample surface roughness responsible for the anomalously large  $H_{c3}$ ? Further studies to elucidate this question are currently underway.

## Acknowledgments

This work was supported by the Israeli Ministry of Science (Israel–Ukraine and Israel–Russia funds), and by the Klatchky Foundation for Superconductivity. We wish to thank I Felner, Ya Kopelevich and A E Koshelev for fruitful discussions. Help with programming provided by W Glaberson is gratefully appreciated.

**References**

- [1] Saint-James D and de Gennes P G 1963 *Phys. Lett.* **7** 306  
de Gennes P G 1966 *Superconductivity of Metals and Alloys*  
(New York: Benjamin)
- [2] Hempstead C F and Kim Y B 1964 *Phys. Rev. Lett.* **12** 145
- [3] Tomasch W J and Joseph A T 1964 *Phys. Rev. Lett.* **12** 148
- [4] Strongin M, Paskin A, Schweitzer D G, Kammerer O F and  
Craig P P 1964 *Phys. Rev. Lett.* **12** 442
- [5] Burger J P, Deutscher G, Guyon E and Martinet A 1965 *Phys.*  
*Rev.* **137** A853
- [6] Rollins R W and Silcox J 1967 *Phys. Rev.* **155** 404
- [7] Hart H R Jr and Swartz P S 1967 *Phys. Rev.* **156** 403
- [8] Akhmedov S Sh, Karasik V R and Rusinov A I 1969 *Zh. Eksp.*  
*Teor. Fiz.* **56** 444  
Akhmedov S Sh, Karasik V R and Rusinov A I 1969 *Sov.*  
*Phys.—JETP* **29** 243 (Engl. Transl.)
- [9] Kulik I O 1967 *Zh. Eksp. Teor. Fiz.* **52** 1632  
Kulik I O 1967 *Sov. Phys.—JETP* **25** 1085 (Engl. Transl.)
- [10] Mathieu P, Plaçais B and Simon Y 1993 *Phys. Rev. B* **48** 7376
- [11] Mathieu P and Simon Y 1988 *Europhys. Lett.* **5** 67
- [12] Kötzler J, von Sawilski L and Casalbuoni S 2004 *Phys. Rev.*  
*Lett.* **92** 067005
- [13] Scola J, Pautrat A, Goupil C, Mechin L, Hardy V and  
Simon Ch 2005 *Phys. Rev. B* **72** 012507
- [14] Tsindlekht M I, Genkin V M, Leviev G I, Felner I, Yuli O,  
Asulin I, Millo O, Belogolovskii M A and Shitsevalova N Yu  
2008 *Phys. Rev. B* **78** 024522
- [15] Shoenberg D 1984 *Magnetic Oscillations in Metals*  
(Cambridge: Cambridge University Press)
- [16] Lortz R, Wang Y, Tutsch U, Abe S, Meingast C, Popovich P,  
Knafo W, Shitsevalova N, Paderno Yu B and Junod A 2006  
*Phys. Rev. B* **73** 024512
- [17] Leviev G I, Genkin V M, Tsindlekht M I, Felner I,  
Paderno Yu B and Filippov V B 2005 *Phys. Rev. B*  
**71** 064506